

PAPER • OPEN ACCESS

Filters for RFI suppression in AERA radio detection of cosmic rays

To cite this article: Zbigniew Szadkowski and Pierre Auger Collaboration 2019 *J. Phys.: Conf. Ser.* **1181** 012078

View the [article online](#) for updates and enhancements.



IOP | ebooks™

Bringing you innovative digital publishing with leading voices to create your essential collection of books in STEM research.

Start exploring the collection - download the first chapter of every title for free.

Filters for RFI suppression in AERA radio detection of cosmic rays

Zbigniew Szadkowski

Faculty of Physics and Applied Informatics, Department of High-Energy Astrophysics, 90-236 Łódź, Poland, tel: +48 42 635 56 59

E-mail: zbigniew.szadkowski@fis.uni.lodz.pl

for the Pierre Auger Collaboration

Observatorio Pierre Auger Av. San Martn Norte 304, 5613 Malarge, Argentina,
Full author list: http://www.auger.org/archive/authors_2018_07.html

E-mail: auger_spokespersons@fnal.gov

Abstract.

Radio stations can observe radio signals caused by coherent emissions due to geomagnetic radiation and charge excess processes mainly in the frequency band from 30 to 80 MHz. This range is often highly contaminated by human-made RFI. In order to improve the signal to noise ratio, RFI filters have to suppress this contamination.

The paper compares several (currently in use and proposed) RFI filters used in the Auger Engineering Radio Array (AERA), being a part of the Pierre Auger Observatory. We analyzed both: the non-adaptive filter (IIR notch) as well as adaptive filters: IIR notch supported by the virtual NIOS[®] processor, FIR based on the linear prediction supported by the virtual NIOS[®] processor, the FIR fully implemented into FPGA fabric used the Levinson algorithm without any processor (all coefficients fully calculated in the FPGA logic elements) and finally the Delayed Least Mean Square filter also with a modification proposed by Harris, variable step size and Instantaneous LMS filter.

We investigated: the efficiency of the several mono-carriers suppression, the distortion factors of cosmic rays pulses after filtering, the speed of the filter response as well as the power consumption crucial for systems supplied by solar panels.

The 200 MW solar farm with 250 kV power line is anticipated to be built in the Southern part of the Auger array. High-power DC/AC converter for sure introduce a huge noise in the electromagnetic spectrum being a topic of interest of AERA. Very efficient, adaptive filter becomes a crucial issue. Simulations and laboratory measurement suggest that the most promising will be the Instantaneous Least Mean Square filter with dynamically modified input range.

1. Introduction

Particles coming from the Universe with ultrahigh energy, known as cosmic rays (UHECRs), penetrate the Earth's atmosphere and generate avalanches of charged and neutral particles known as Extensive Air Showers (EAS) discovered in the late 1930s [1]-[5]. The origin of UHECRs still remains a mystery. Several experiments (e.g. the Pierre Auger Observatory



[6]) investigate EAS to estimate the energy, arrival direction of each cosmic ray as well as to analyze a distribution of primary masses (cosmic ray composition).

Radio detection of EAS started in the 1960s [7]. In the last decade, the LOPES [8] and CODALEMA [9] Collaborations continued radio detection together with other radio array, such as LOFAR [10] and Tunka-Rex [11]. The Auger Engineering Radio Array [12]-[13] is the radio detector in the Pierre Auger Observatory (together with the fluorescence and surface ones) to measure EAS with an energy larger than 10^{17} eV.

The geomagnetic radiation [14] and the Askaryan charge-excess [15] are the main responsible for the radio emission. The geomagnetic effect is a consequence of the induction of a transverse electric current in the shower front generated by the Earth's magnetic field. The charge excess in the shower front is to a large extent due to the knock-out of fast electrons from the ambient air molecules by high-energy photons in the shower. The refractive index of the air is slightly bigger from unity. This causes a Cherenkov-like time compression [16], which affects both the radiation mentioned above.

The crucial condition for a radio detection is the radio signals coherence, which is investigated in a frequency range of 30 - 80 MHz (analog electronics uses a band-pass filter). The coherence appears also above 80 MHz, but the upper coherence frequency depends strongly on the distance to the shower axis reaching even GHz frequencies. Additionally, 80 MHz cut-off removes also the FM radio band. The lower frequencies usually reflect frequently in the atmosphere, so detectors can register emission from very distant storms. The lower limit is optimized for the signal-to-noise ratio of EAS pulses vs. Galactic noise. The selected frequency band contains mostly Galactic noise and human-made RFI. In order to assure a high quality self-trigger, radio signals should be cleaned from RFI.

2. Filters currently in use and proposed

The environment is mostly contaminated by narrow-band mono-carriers of short-wave transmitters. The narrow peaks in the frequency domain have to be strongly suppressed before the trigger is generated. The improvement of the signal to noise ratio is crucial to avoid spurious triggers and a registration of empty events. The AERA used two types of the RFI filters:

- **1)** an adaptive one based on the FFT conversion from time to frequency domains filtered afterwards by the median filter and the second conversion from the frequency to the time domain by the Hilbert transform [18].
- **2)** a non-adaptive IIR notch filter with fixed coefficients [17], which suppress four narrow bands. Coefficients calculated in an external C program have been implemented into the FPGA code as constants [17]. If the frequencies of the contaminations are stable (e.g., correspond to short-wave transmitter carriers) a non-adaptive filter is very efficient. However, if the frequencies of contamination do not match the IIR coefficients, the IIR filter is practically useless: the output signals are approximately the same as the input ones.

The adaptive FFT-Median-iFFT filter (**1**) was installed in the first generation of radio stations with Cyclone[®]III FPGA and 180 MHz sampling frequency. The relatively low frequency of the ADC clock (providing a relatively narrow safety margin to the Nyquist condition) was a consequence of used over-clocking necessary to avoid aliasing. Even the fastest Cyclone[®]III FPGA did not allow on higher clock frequency. Two polarization channels would require straightforward to use two FFT engines for calculating the frequency domain signal, while setting their imaginary input to zero. A trick was used, two channels were connected to a single FFT engine (real and imaginary inputs), outputs were next disentangled to the Fourier components. Although the FFT approach was working correctly, it has not been implemented in the second generation design with Cyclone[®]IV due to high power consumption and very complicated FPGA code.

The non-adaptive IIR notch filter (2) were implemented in the next generation of electronics - in radio stations with Cyclone[®]IV and 200 MHz sampling frequency. Adaptive filters allowing an RFI suppression independently of the frequencies of the contamination, are more flexible than non-adaptive filters with fixed parameters usually tuned for the local transmitter frequencies. Such a solution is efficient: however, it cannot react to any additional RFI sources. Nevertheless, for well defined short-wave carriers in AERA region the IIR filter has been working extremely efficient and with very low power consumption. If the risk of contamination by the solar farm is low, the IIR filter would be still the best solution.

A proposed filter was already tested in Argentinean pampas:

- **3a)** The adaptive 32-stage FIR filter based on the linear prediction (LP) of the signal supported by the NIOS[®] processor. The NIOS[®] processor had to solve 32 linear equations in the FPGA. Calculations in the NIOS[®] provided the same precision as in the Microsoft Visual C++. This filter was tested in real Argentinean pampas conditions and proved its efficiency and stability [19][20]. Coefficients calculation in the NIOS[®] processor take ~ 600 ms. This refresh time is considered too long. The filter cannot react on short-time spikes.

The filter **3a)** fulfilled our expectations, however further work was done and new filters with interesting and promising features are proposed:

- **3b)** The variant with the Hardcore Processing System, with embedded micro-controller in the FPGA. The design was developed on Cyclone[®]V SoC Development Kit and SoC Embedded Design Suite with 5CSXFC6D6F31C6N (SoC) FPGA. FIR coefficients are calculated in the embedded micro-controller with 925 MHz clock (instead of 100 MHz in NIOS[®] allowed decreasing the refresh time from ~ 600 ms to ~ 20 ms only. This design as it required FPGA with SoC could not be tested in the field. Its feature was the same as **3a)** with 30 times shorter calculation of FIR coefficients.
- **3c)** The linear prediction method generates the auto-covariance Toeplitz matrix calculated from ADC samples. Linear equations are next solved by much faster Levinson procedure instead of relatively slow Gaussian elimination. The algorithm of solving 32 linear equations based on the Levinson procedure has been implemented directly in the FPGA fabric [22]. The refresh time was only $\sim 600 \mu\text{s}$. Implementation of parallel processes directly in the FPGA fabric reduces the refresh time. However, it increases the power consumption, a crucial factor for applications supplied from solar panels. This variant will be tested in the field, especially in seriously contaminated regions.
- **4a)** The adaptive Normalized Least Mean Square (NLMS) filter with a canonical FIR section [23]. This is the first design based on the LMS approach. It is relatively slow as using a division operation for a normalization. Unfortunately, the Altera Mega-function implementing a division operation does not use the fast multipliers from DSP blocks. In order to assure a sufficient speed of 200 MHz (required for ADCs) the length of the FIR filter should not be longer than 16. It seems to be too short.
- **4b)** The adaptive Delayed Least Mean Square (DLMS) filter with non-canonical FIR section [24]. It is significant modification of the NLMS algorithm without any division operation. It provides much faster registered performance and allows an implementation of 32- or 64-stage FIR.
- **4c)** The DLMS modification with variable step size [26] proposed by Harris [25]. Laboratory measurements did not confirm a superiority of variable step approach in comparison to the fixed learning factor design.
- **4d)** The Instantaneous LMS modification (ILMS) without a delay line as in the DLMS design. An analysis showed that the DLMS algorithm distorted cosmic rays signal introducing echoed artifacts. Removing a delay line significantly improved the shape of

signal after filtering. The most efficient filtering is for very large contaminated signal. The investigated cosmic ray signals deeply hidden in the background are very efficiently extracted from the noise.

- 4e) The ILMS algorithm can perfectly extract signals from a large noise but it does not show so high efficiency for smaller contamination. In order to improve the RFI suppression also for relatively low RFI levels, the dynamical shift of the ADC input has been proposed (an artificial amplification and reduction after filter). This LMS variant seems to be most optimal and will be tested in the field.

3. Suppression efficiency

The suppression efficiency has been tested with four mono-carriers, a condition the IIR notch filter was optimized for. Selected frequencies were as follows: 29.17, 41.11, 59.37 and 72.43 MHz, respectively. Amplitudes were tuned to be at a similar level.

3.1. IIR notch filter

The IIR notch filter was tested for 4 frequencies of mono-carriers (Figure 1A) exactly matching the assumed condition of perfect suppressions (Figure 1b) and with a single frequency evidently out of the suppression window (Figure 1c). If at least a single mono-carrier does not match the optimal IIR notch suppression window, a full filter is practically useless. For this mono-carrier the IIR notch filter is practically transparent and a suppression of the rest of mono-carriers does not matter. However, if all frequencies of mono-carriers match the assumed coefficients the RFI suppression is extremely efficient (spectral amplitudes are suppressed by a factors of $\sim 30 - 100$).

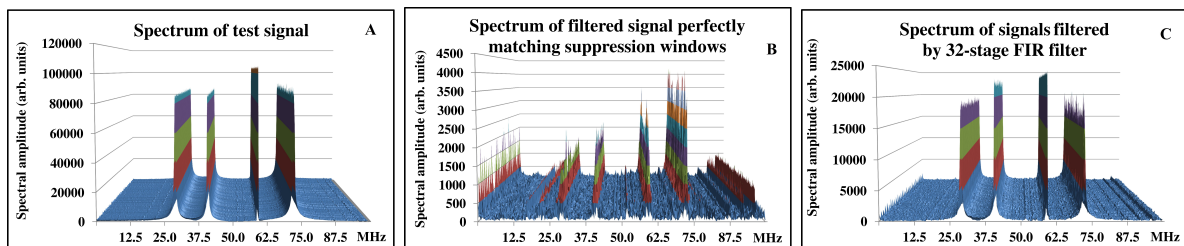


Figure 1. Spectra of signals: original from 4 external generators (test signal with 4 carriers with 29.17, 41.11, 59.37 and 72.43 MHz, respectively - left plot: A), filtered by the IIR notch filter with perfectly matching of all frequencies for a maximal suppression (middle plot: B) and filtering by the LP FIR filter (right plot: C).

3.2. FIR filter based on the linear prediction

The 32-stage FIR filter based on the linear prediction [19] has been successfully tested in Argentinean pampas [20]. In comparison to IIR notch filter its suppression efficiency is much smaller (Figure 1C) - the suppression factors are at the level of ~ 5 while for IIR notch filter the suppression factors are above 20 and sometimes reach even ~ 100 . The main advantage of the FIR filter is its adaptivity, which allows a suppression of either new sources or the same source with moved frequency. Adaptive filters are especially useful in environment with non-stationary RFI sources.

The filter based on the hardware implementation of the Levinson procedure directly into the FPGA fabric will not be analyzed as it is based on the same algorithm which does not provide a sufficient RFI suppression. The filter with Levinson algorithm implemented directly in the FPGA fabric is much faster than FIR filter supported by the NIOS[®] processor, but the power consumption is much higher due to parallel processing and much bigger resources occupation.

3.3. LMS32 filters

The NLMS filter solves the problem of normalizing by the learning factor updated in every iteration. The division operation requires a 24-stage pipeline LPM_DIVIDE Mega-function, which is rather slow since it is not supported by DSP blocks as multipliers. The filter uses the canonical FIR section requiring additionally 5 pipeline stages for a 32-stage length.

Much faster than using the non-canonical FIR algorithm is the DLMS32 filter showing a very good suppression efficiency, practically for all allowed learning factors. Optimization of the DLMS32 for elimination echoed artifacts removed the delay line. The ILMS32 provides the same suppression features as the DLMS32 (Figure 2). Variable step size LMS [25][26] as nor indicating superiority than the fixed learning factor approach are not developed anymore. The last design and most promising, the ILMS32 with dynamical input range (VRILMS) seems to be the the optimal for very wide range of potential contaminations [27].

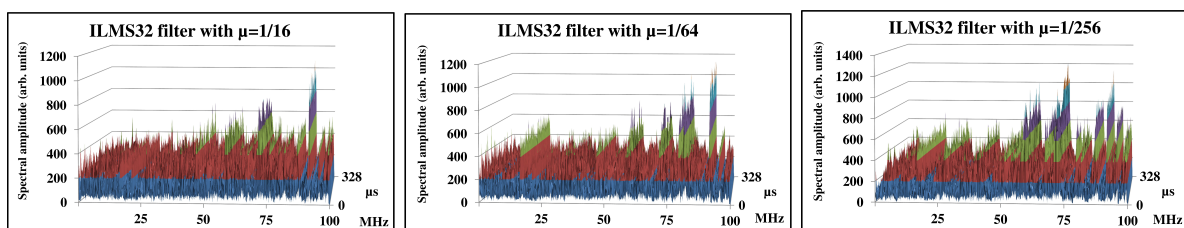


Figure 2. Spectra of signals filtered by the 32-stage DLMS filter with various learning factors.

4. Distortion factors

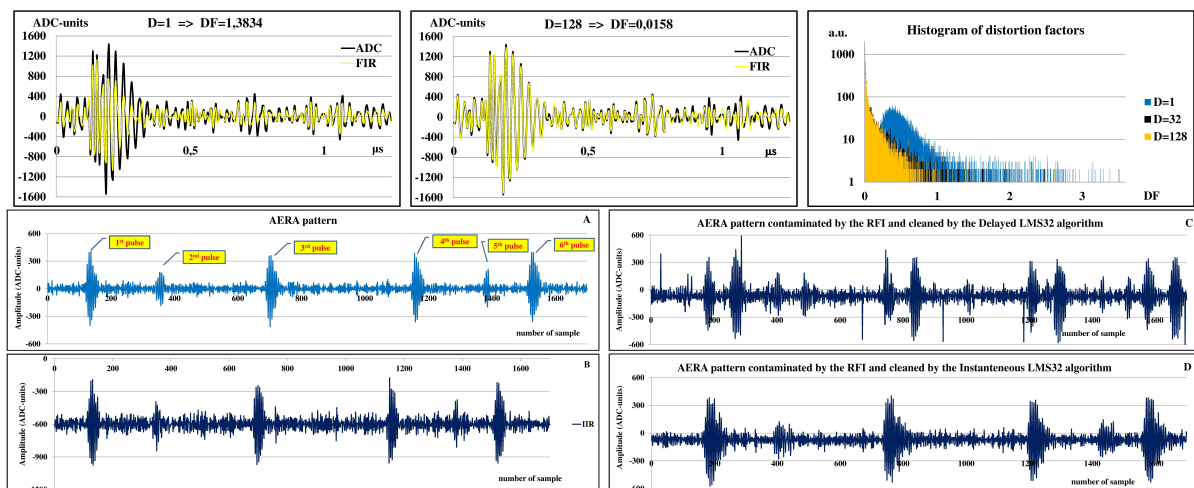


Figure 3. Example of signal more or less distorted depending on the length of the delay line for the LP FIR filter (the first row) and six original AERA pulses (A) contaminated by four sine RFI and next cleaned the IIR filter (B), the DLMS (C) and the ILMS algorithms (D).

Distortion factors in the LP FIR filter were reduced by an adjustment of the delay line length to $D=128$. However, this approach for the LMS filters shows echoes signals. The minimum of distortion factors was obtained in the case of absence of any delays. Figure 3 shows an example of real AERA events contaminated artificially by four mono-carriers and next cleaned by IIR, DLMS and ILMS filters. The IIR provides the minimal distortion factors, however, the ILMS algorithm assures a sufficiently good signal reconstruction for the self trigger circuit.

5. Power consumption

As expected, the IIR filter shows the lowest power consumption for both FPGAs. However, Cyclone[®] V indicates rather a large static power dissipation. For potentially future applications Cyclone[®]10 is definitely the favorite. Unexpectedly, the power consumption for VRILMS32 is twice bigger than for the FIR32 (for Cyclone[®]10). Let us notice that the power consumption for Cyclone[®]10 and Cyclone[®]IV E are comparable. This simplifies tests in real pampas conditions where EP4CE75F29C6 FPGA is now used (Figure 4).

Power in mW	EP4CE75F29C6				5CEFA9F3117				10CL120YF78017G			
	IIR	FIR32	Levinson	VRILMS	IIR	FIR32	Levinson	VRILMS	IIR	FIR32	Levinson	VRILMS
Total Thermal Power Dissipation	152.8	189.6	297.8	361.3	543.8	772.3	1134.9	739.9	140.1	170.7	280.8	362.9
Core Dynamic Thermal Power Dissipation	19.2	39.2	146.1	215.0	15.2	200.4	562.4	172.9	24.2	39.1	148.1	228.3
Core Static Thermal Power Dissipation	90.9	95.2	97.7	91.7	518.7	527.9	530.3	521.1	74.4	78.1	80.0	75.2
I/O Thermal Power Dissipation	42.7	55.2	54.1	54.7	10.0	44.0	42.3	45.9	41.5	53.5	52.7	59.4

Figure 4. Power consumption for various filters and three FPGAs from Cyclone[®]IV E, Cyclone[®]V and Cyclone[®]10 families estimated by the Quartus[®] Power Analyzer Tool.

6. Conclusions

The analysis of the RFI filters shows that the most promising for the future working in an very contaminated environment is the VRILMS32 based on the Cyclone[®]10 FPGA.

References

- [1] Rossi B 1934 *Supplemento a la Ricerca Scientifica* **1** 579.
- [2] Schmeiser K and Bothe W 1938 *Annals of Physics* **424** 161
- [3] Kolhörster W, Matthes I and Weber E 1938 *Naturwissenschaften* **26** 576
- [4] Auger P, Maze R and Robley A F 1939 *Comptes Rendus* **208** 1641
- [5] Auger P, Ehrenfest P, Maze R, Daudin J and Robley A F 1939 *Rev. of Modern Physics* **11** 288
- [6] Aab A et al., (Pierre Auger Collaboration) 2015 *Nucl. Instrum. Meth.* A798 (2015) 172.
- [7] Allan H R 1971 *Progress in Part. and Nucl. Phys: Cosmic Ray Physics (North-Holland Publishing Company (Amsterdam))* **10**, 169
- [8] Falcke H et al. 2005 *Nature (London)* **435** 313
- [9] Ardouin D et al. 2006 *Astropart. Phys.* **26** 341
- [10] Schellart P et al. (LOFAR Collaboration) 2013 *Astron. Astrophys. A* **98** 560
- [11] Bezyazeev P A et al., (Tunka-Rex Collaboration) 2015 *Nucl. Instrum. and Meth. A* **802** 89.
- [12] Huege T (Pierre Auger Collaboration) 2010 *Nucl. Instrum. Meth. A* **617** 484
- [13] Aab A et al. (Pierre Auger Collaboration) 2012 *JINST* **7** P10011, 2016 *JINST* **11** P01018
- [14] Kahn F D and Lerche I 1966 *Proc. of the Royal Society of London Series A-Math. and Phys, Sci.* **289** 206
- [15] Askaryan G A 1962 *Sov. Phys. JETP* **14** 441
- [16] James C W, Falcke H, Huege T and Ludwig M 2011 *Phys. Rev. E* **84** 056602
- [17] Kelley J L for the Pierre Auger Collaboration 2013 *Nucl. Instrum. Meth. A* **725** 133
- [18] Schmidt A, Gemmeke H, Haungs A, Kampert K-H, Rühle C and Szadkowski Z 2011 *IEEE Trans. on Nucl. Science* **58** 4 1621
- [19] Szadkowski Z, Fraenkel E D and van den Berg A M 2013 *IEEE Trans. Nucl. Science* **60** 5 3483
- [20] Szadkowski Z, Głaś D, Timmermans C and Wijnen T for the Pierre Auger Collaboration 2015 *IEEE Trans. Nucl. Science* **62** 3 977
- [21] Szadkowski Z and Głaś D 2016 *IEEE Trans. Nucl. Science* **63** 3 1455
- [22] Szadkowski Z 2017 *IEEE Trans. Nucl. Science* **64** 11 1455
- [23] Szadkowski Z and Głaś D 2017 *IEEE Trans. Nucl. Science* **64** 6 1304
- [24] Szadkowski Z and Szadkowska A 2018 *Real-Time and Embedded Systems and Technologies (RTEST) (Tehran)* DOI: 10.1109/RTEST.2018.8397081
- [25] Harris R W et. al, 1986 *IEEE Trans. on Acoustics, Speech and Signal Processing* **ASSP-34(2)** 309
- [26] Szadkowski Z 2018 *International Conference on Advances in Big Data, Computing and Data Communication Systems (icABCD 2018) (Durban)*
- [27] Szadkowski Z 2018 submitted to *IEEE Trans. Nucl. Science*